Neuroendocrine Tumors of the Pancreas: Diagnosis

Jun Ushio[1], Kensuke Yokoyama[1], Alan Kawarai Lefor[2], Kiichi Tamada[1]

[1]Division of Gastroenterology, Department of Medicine, Jichi Medical University, Japan
[2]Department of Surgery, Jichi Medical University, Japan

ABSTRACT

Pancreatic neuroendocrine tumors are rare. In patients with functional PNETs, the excess hormones produced lead to a variety of hormone-related symptoms. Non-functioning tumors do not produce symptom-inducing hormones. Therefore, they are often discovered at an advanced stage with large tumors and metastatic spread. PNETs have a variable appearance on computed tomography scans and magnetic resonance imaging. With most functioning PNETs, Dynamic computed tomography scans and magnetic resonance imaging show well defined hypervascular small tumors. Imaging of other types of PNET show purely cystic, complex cystic or solid tumors. Functional imaging is useful both to detect the primary lesion and stage the disease. It is also useful to select candidates for peptide receptor radiometabolic treatment. Somatostatin receptor scintigraphy is the most available functional imaging technique. The gallium 68-SST analogue positron emission tomography scan is more sensitive, and is expected to be the future of functional imaging for PNETs. 18FDG PET/CT scan is useful for poorly differentiated tumors. The sensitivity of Carbidopa-assisted 18F-FDOPA PET/CT is better than somatostatin receptor scintigraphy for detecting nonfunctional PNETs. Endoscopic ultrasonography is superior to dynamic computed tomography scan to identify PNETS. Endoscopic ultrasonography-fine needle aspiration offers a high accuracy for the diagnosis of PNETs. However, tumors located in the pancreatic head and tumors with rich stromal fibrosis are associated with reduced sampling adequacy of endoscopic ultrasonography-fine needle aspiration. Some patients with poorly-differentiated PNETs have invasion of the pancreatic duct. Endoscopic retrograde cholangiopancreatography is useful for evaluating these patients.

INTRODUCTION

Pancreatic neuroendocrine tumors (PNETs) are a rare group of heterogeneous neoplasms [1, 2, 3]. PNETS can be classified as either functional or non-functional according to the presence of biologically active hormones and characteristic symptoms. PNETS show a wide range of malignant potential which range from slow-growing and non-infiltrative tumors to locally invasive and metastasizing tumors. Significant advances in diagnostic modalities have been made over the past decade. Although many reviews describe the utility of cross-sectional imaging modalities, the utility of endoscopic modalities in this area has not been well discussed. This article provides a comprehensive review of PNETs and an update on advances in this area.

CLINICAL AND BIOLOGICAL PRESENTATION

Functional PNETs

Received December 1st, 2017 - Accepted December 22nd, 2017
Keywords Neuroendocrine Tumors; Pancreas
Abbreviations CEUS contrast-enhanced ultrasonography; MEN multiple endocrine neoplasia; PNETs pancreatic neuroendocrine tumors
Correspondence Jun Ushio
Department of Medicine
Division of Gastroenterology
Jichi Medical University
3311-1 Yakushiji, Shimotsuke
Tochigi 329-0498, Japan
Tel +81 285 58 7348
Fax +81 285 44 8297
E-mail j.ushio@jichi.ac.jp

Some PNETs are functional. The excess hormones produced lead to a variety of hormone-related symptoms **(Table 1).** In these patients, early diagnosis is often possible even if the tumor is small.

Approximately 60% of functioning PNETs are insulinomas, which are usually benign. Other types of PNETs are often malignant. Whipple's triad is famous as the constellation of symptoms in patients with insulinomas, and includes the presence of symptomatic hypoglycemia (in about 85% of patients), low blood sugar at the time of symptoms, and relief of symptoms with glucose administration. Therefore, many patients are obese due to overeating to avoid hypoglycemia.

Gastrinomas are gastrin-secreting tumors with symptoms typical in common peptic ulcer disease. Usually, the abdominal pain is less responsive to medical treatment. Sometimes, symptoms may relate to a complication of peptic ulcer disease, such as bleeding, gastric outlet obstruction, or perforation. Over 50% of gastrinomas are malignant. They may metastasize to regional lymph nodes and the liver. Hypergastrinemia also occurs in patients taking a proton pump inhibitor, especially with chronic renal failure as well as patients with gastrinomas. Expensive diagnostic evaluations for gastrinoma should not be conducted in these patients. Twenty percent of gastrinomas are related to multiple endocrine neoplasia (MEN) type-1 and are associated with hyperparathyroidism and pituitary adenomas. Patients with MEN type-1 associated PNETs are usually diagnosed at an earlier age than sporadic tumors. Clinical symptoms

Table 1. Subtypes of functioning PNETs classified by the secreted hormone.

Subtype	Percentage	Secreted hormone	Rate of malignancy	Clinical symptoms due to hormone
Insulinoma	40%-60%	Insulin	< 10%	Hypoglycemia
Gastrinoma	20%-50%	Gastrin	60%-90%	Peptic ulcer Gastroesophageal reflux disease, diarrhea
Glucagonoma	Rare	Glucagon	50%-80%	Necrolytic migratory erythema, diabetes, venous thrombosis, depression
Somatostatinoma	Rare	Somatostatin	> 70%	Diabetes, hypochlorhydria, cholelithiasis, diarrhea
VIPoma	Rare	Vasoactive Intestinal Peptide	40%-70%	Watery diarrhea, hypokalemia, achlorhydria

associated with other functioning tumors are summarized in **Table 1**.

Nonfunctional PNETs

Non-functioning tumors do not produce hormones, and are generally asymptomatic. Therefore, they are often discovered in an advanced stage with large tumors which have already metastasized at the time of diagnosis. Symptoms in patients with non-functioning PNETs are non-specific, and include abdominal pain, diarrhea, a prolonged feeling of fatigue, fainting, or weight loss. More than 50% of non-functioning tumors (about 40% of PNETs) are likely to be malignant (metastatic potential).

CROSS-SECTIONAL IMAGING

Ultrasonography (US)

The utility of conventional ultrasonography for the diagnosis of PNETs is limited, since it has limited ability to image the tail of the pancreas, especially in obese patients. However, recent studies have reported the utility of contrast-enhanced ultrasonography (CEUS) in this area. CEUS shows slightly, moderately or well-enhanced patterns in patients with pancreatic adenocarcinoma, inflammatory pancreatic masses, and islet cell tumors, respectively [4]. The imaging pattern on CEUS correlates with tumor grade (G1 and G2) except for G3 lesions in patients with PNETs. These findings support a possible role for information from CEUS to be used as a prognostic factor [5].

Computed Tomography (CT) Scan

Primary Tumor: CT is the main imaging modality for PNETs. For evaluation of PNETs, arterial/pancreatic phase, venous phase and delayed phase are required. The late arterial (30 s) or pancreatic phase (40 s) is suitable for the detection of small functioning PNETs in particular insulinoma [6]. It is also suitable for the detection of hepatic metastases [6, 7, 8, 9]. In our experience, however, only early arterial phase shows tumor in some patients with small functioning PNETS. The delayed phase is complementary to the arterial/pancreatic and the venous phase. Delayed phase CT scan shows delayed enhancement in some fibrous tumors [10].

Functioning Tumors: Functioning PNETs are most often manifest by endocrine symptoms. Therefore, the tumors can be detected early, often when they are small.

Insulinomas are most frequent among the functioning PNETs. Most insulinomas are under 2cm in size, solitary and benign. These tumors are detected throughout the pancreas including the head, body, and tail. Typical insulinomas are hyper-vascular and CT scans show intense enhancement during the early phase (arterial/pancreatic) **(Figure 1)**. The enhancement is usually uniform. Sometime, a rim of enhancement is seen [11].

Gastrinomas are the second most common among PNETs. Gastrinomas are also small pancreatic tumors generally 1-3 cm. About 80% are found within the ''gastrinoma triangle'' defined as the confluence of the cystic and common bile duct superiorly, the second and third portions of the duodenum inferiorly, and the neck and body of the pancreas medially. Gastrinomas also are often associated with MEN1 syndrome. In gastrinomas, dynamic CT scans often show a delayed enhancement persistent in the delayed phase due to the presence of fibrosis.

CT scan imaging of other functioning PNETs includes purely cystic tumors in 10%, a common pattern of PNETs associated with MEN1, and complex solid and cystic appearance and calcified tumors in less than 5% **(Figure 2)** [12].

The differential diagnosis of hypervascularized PNETs includes pancreatic metastases from a renal cell carcinoma and an intrapancreatic accessory spleen. In addition, pancreatic arterio-venous malformations also have an appearance similar to small hypervascularized PNETs. CT scan findings in patients with pancreatic metastases from renal cell carcinoma and patients with hypervascular PNETs were compared with a focus on the relative percentage washout (RPW). The mean RPW in the renal cell carcinoma group was significantly higher than that in the PNET group [13]. Multiple hypervascular PNETs is frequently seen in patients with MEN1 as well as in those with metastases from renal cell carcinoma.

Non-Functioning Tumors: On CT and MR imaging, non-functioning PNETs are seen as large pancreatic masses with heterogeneous enhancement because of necrotic and hemorrhagic changes. Patients with hypo-enhancing tumors **(Figure 3)** generally have a worse prognosis after resection compared to patients with hyper-enhancing

Figure 1. Hyper-enhancing tumor (Insulinoma, G1). **(a, b).** Computed tomography scan images in the transverse plane during the arterial and the portal venous phase show a small hyper-vascularized tumor in the pancreas with sharp margins. **(c).** T2-weighted magnetic resonance image shows a small lesion with a well circumscribed margin and high signal intensity.

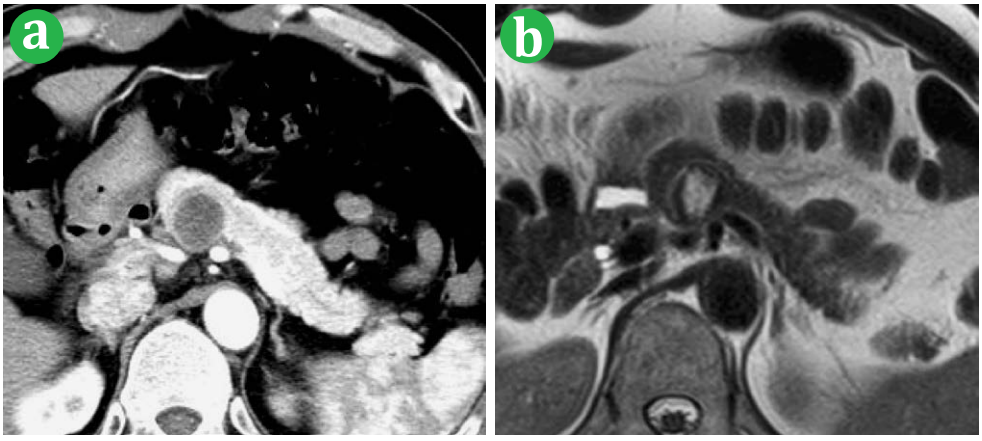

Figure 2. Cystic and hyperenhancing tumor (Non-functional tumor, G2). **(a).** A Dynamic computed tomography scan image obtained during the arterial phase shows a large mass with solid and cystic components. **(b).** A T2-weighted magnetic resonance image shows a small lesion with high signal intensity.

lesions or a cystic appearance with hyper-enhancing tumors [14].

Staging: CT scan plays a major role in the staging of these lesions. The TNM stage and the extent of distant metastases, especially to the liver, are the most important prognostic factors. Liver metastases correlate with the prognosis [15, 16] and are important parameters in developing the optimal treatment plan. Other typical sites for metastases from PNETs include abdominal and mediastinal lymph nodes, peritoneum, and bone. The frequency of metastatic disease in each of these sites depends on the biologic behavior of the primary tumor, the stage of disease and differentiation of the primary tumor [17].

CT scan and somatostatin receptor scintigraphy (SRS) complement each other for the staging of PNETs. While CT scan is more sensitive for detecting lung, liver and brain metastases, SRS is more sensitive for detecting metastases to bones and the mediastinum [9, 18, 19].

Magnetic Resonance (MR) Imaging

Primary Tumor: MR imaging protocols for PNETs should include T1-(T1W) and T2- weighted (T2W) sequences, dynamic three-dimensional (3D) sequences before and after intravenous administration of a gadolinium chelate with multi-arterial, venous and delayed over 5 min acquisition and diffusion-weighted (DWI) sequences. Fat suppression on T1W and T2W images is useful to maximize the signal intensity differences between the pancreatic tumor and the adjacent normal pancreatic tissue. Similar to CT scan, T1W images delayed over 5 min images improve tumor detection [10]. Diffusion-weighted images increase the sensitivity to detect the primary pancreatic tumor as well as associated liver metastases [20].

Functioning Tumors: In most functioning PNETs, MRI shows low signal intensity on T1W, high signal intensity on T2W images and intense and early enhancement on dynamic T1W sequences. The T2W sequence with fat suppression is useful to detect hypervascular tumors (typically, insulinoma). However, hypovascular tumors are better detected using the T1W sequence during the arterial phase. Non-hypervascular tumors are surrounded by enhanced normal pancreatic parenchyma. Therefore, strong enhancement of the pancreas in the arterial phase is suitable to detect it. This condition may conceal hypervascular tumors [21].

DWIs are useful to show small PNETs due to their excellent image contrast. ADC values are lower than adjacent pancreatic parenchyma in all cases of solid nodules [21]. However, ADC values are higher in the presence of a cystic pattern [22].

Non-Functioning Tumors: On MR images, most PNETs are hyperintense on T2W images and hyper- or isointense during the arterial/pancreatic phase of a dynamic study

in contrast to pancreatic adenocarcinoma [23]. Tumor vein thromboses (splenic, portal and superior mesenteric veins) are frequent, and vascular invasion is less common with PNETs compared to pancreatic adenocarcinoma [21, 23] **(Figure 3)**. Dilatation of the upstream pancreatic and common bile duct is also less common than in pancreatic adenocarcinoma [24].

Staging: MRI is more sensitive than US, CT scan, or SRS for the detection of liver metastases. It is also the imaging technique with the best inter-observer agreement [7, 8] **(Figure 3)**. Its sensitivity is similar to that of intraoperative US. However, available pre- and intraoperative imaging techniques cannot detect about half of all liver metastases [25]. The addition of DWI sequences to standard MRI revealed additional metastases and led to modifications in patient management. Adding DWI to standard liver MRI provided additional findings for 45% of patients with 1.78 times more new lesions, and resulted in a management change for 18% of patients. DWI sequences added to whole body MRI provided additional findings for 71% of patients, with 1.72 times more lesions, resulting in a management change for 19% of patients [26].

RADIOPHARMACEUTICAL IMAGING TECHNIQUES

Somatostatin Receptor Scintigraphy (SRS)

Isotope-imaging modalities have a major role in the management of patients with PNETs. Due to the expression of multiple somatostatin receptors (SSTRS) by about 70% of PNETS, functional imaging with somatostatin (SST) analogues is used to detect NETs [27]. Functional imaging with somatostatin analogues is useful first to evaluate the expression of SSTRS. It allows us to assess disease staging,

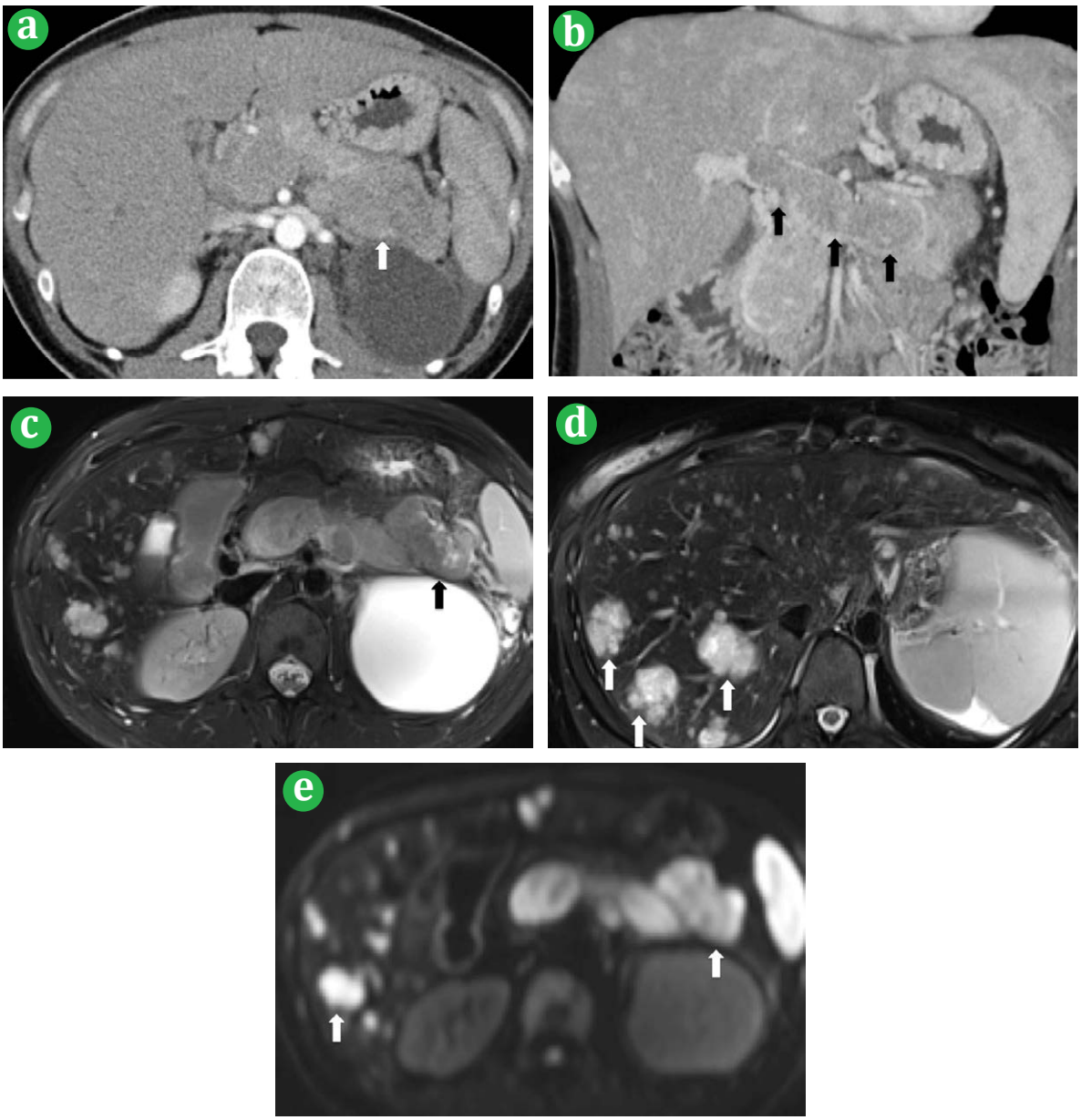

Figure 3. Hypo-enhancing tumor (Non-functional tumor). **(a).** Computed tomography images during the arterial phase show a hypovascularized tumor of the pancreas as shown in pancreatic adenocarcinoma. The lesion has a worse prognosis compared with hyperechoic or cystic and hyper-enhancing tumors. **(b).** Computed tomography images during the portal venous phase show a tumor thrombus in the portal vein. **(c).** Magnetic Resonance images: A T2-weighted image shows a heterogenous hyperintense tumor. **(d).** Magnetic Resonance images: A T2-weighted image shows multiple liver metastases better depicted than on computed tomography scan. **(e).** The pancreatic tumor and liver metastases are also well depicted on diffusion weighted images.

recurrence, and finally to select patient candidate for peptide receptor radio-metabolic treatment (PRRT) by Y90 (Yttrium-90) or Lu177 (Lutetium-177) SST analogues. Poorly differentiated neuroendocrine carcinomas have a low expression of SST receptors and functional imaging with SST analogues has a very limited role [28].

111-pentetrotide single photon emission computed tomography (SPECT)-SRS (OCTREOSCAN; Mallinckrodt, St Louis, MO) is the most commonly available somatostatin analog tracer with high affinity for the 2 and 5 subtypes. Scintigraphic imaging require a 2-day protocol for image acquisition (4h and 24h) with whole body 2D (anterior-posterior) evaluation at 24 h. Currently, SPECT images with 3D and fused images are available. This modality has a higher sensitivity than planar images to localize small primary tumors or distant metastases **(Figure 4)**.

SRS scintigraphy may help detect pancreatic primary tumors when cross-sectional imaging and EUS show no lesions. SRS scintigraphy sensitivity ranges from 40% to 70%. SRS is more sensitive in detecting well-differentiated gastrinomas, glucagonomas, VIPomas and non-functioning PNETS.

FDG PET

Conventional FDG PET/CT

Conventional FDG imaging is not considered a good tracer for NETs. Differentiated G1 NETs are most likely to express the SST receptor, to disclose high SSTA uptake and be negative on FDG PET/CT scan. For staging well-differentiated NETs with high Ki67 indices over 10% and the poorly differentiated variants, FDG PET/CT scan is most useful. In patients with well-differentiated NET and Ki67 over 10%, FDG PET/CT showed higher sensitivity compared to Octreoscan and CT scan with a higher number of detected lesions located in the lymph nodes and bone [29]. Furthermore, FDG uptake is an independent prognostic factor for patients with low-grade gastroenteropancreatic NET (GEPNETS) [30].

F-DOPA PET/CT has had excellent performance for staging midgut tumors. However, studies comparing F-DOPA to Octreoscan in non-midgut digestive NETs showed a better performance of somatostatin analogue imaging compared to F-DOPA with a sensitivity of Octreoscan of 75% compared to 25% for F-DOPA PET/CT [31].

Ga68-SSTA PET also seems to be superior to F-DOPA in a small patient series with well differentiated NETs, including PNETs with sensitivity of 96% for Ga68-SSTA PET/CT as opposed to 56% for F-DOPA PET [32, 33]. Ga 68 PET/CT is more sensitive than Octreoscan with sensitivity of 90% to 100% versus 50% to 80% for Octreoscan. It allows for the detection of micrometastases not seen on Octreoscan, especially in the liver and loco-regional lymph nodes [34, 35]. Some studies showed higher sensitivity of Ga68-SSTA PET tracers comparing to CT scan and/or MRI in detecting distant metastases, especially bone metastases in GEPNETs with sensitivity around 95% to 100% for PET and 60% to 80% for CT. However, further studies comparing Ga68 PET and high quality cross-sectional imaging are needed to define the role of each modality [35, 36, 37, 38].

Carbidopa-Assisted FDG PET/CT

The low sensitivity of ^{18}F-FDOPA PET to detect well-differentiated PNETS may be due to their embryologic origin and the high physiologic radiotracer uptake and retention in the mature exocrine pancreas [39, 40]. Carbidopa (CD) is an efficient inhibitor of the peripheral aromatic amino acid decarboxylase (AADC). The administration of CD improves interpretation of ^{18}F- FDOPA PET images by lowering physiologic pancreatic uptake and increasing tumor-to-background uptake ratios [41, 42]. The combination of CD premedication and early acquisition of PET images improves the detection of insulinomas [43, 44].

The sensitivity of CD-assisted ^{18}F-FDOPA PET/CT (90%) is better than that of SRS (68%) for detecting nonfunctional PNETs. Moreover, ^{18}F-FDOPA PET/CT accurately shows nodal metastatic spread than SRS. These data suggest that the utility of CD-assisted ^{18}F-FDOPA PET/CT for non-functioning PNETS when ^{68}Ga-radiolabeled SSA PET is not yet defined [45].

ENDOSCOPY

Endoscopic Ultrasonography

Endoscopic ultrasonography (EUS) is superior to detect PNETs compared to CT scan, MRI and SRS [46].

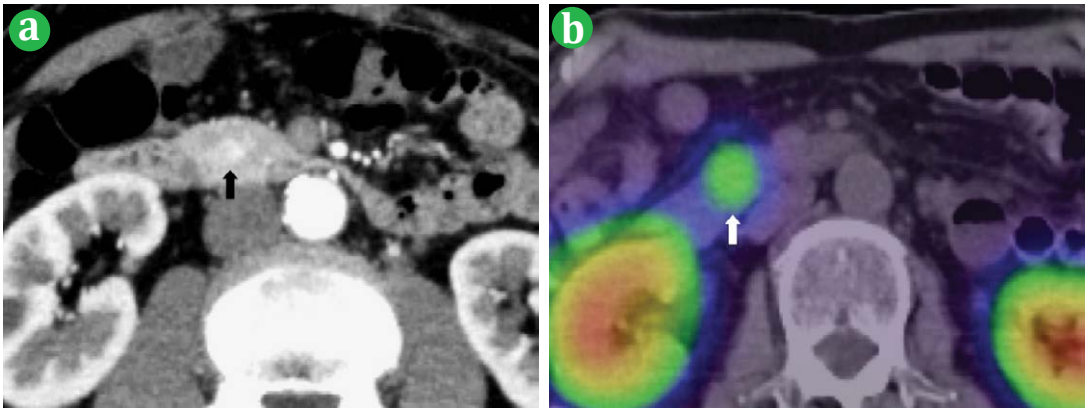

Figure 4. Tumor detected by somatostatin analogue scintigraphy (Insulinoma, G1). **(a).** Dynamic computed tomography scan shows a hypervascular mass. **(b).** 111In-pentetreotide single photon emission tomography (Octreoscan) shows high uptake of somatostatin analogue in pancreas lesions.

EUS is particularly useful to detect small (2 to 5 mm) pancreatic lesions, such as gastrinomas and insulinomas. The detection rates are from 79% to 94% [47, 48, 49] **(Figure 5)**. Due to the proximity of the endoscope, the sensitivity to detect the tumor in the head of the pancreas is higher than in the tail.

Insulinomas are all located in the pancreas with an average size of under 2 cm at the time of diagnosis in 90% of patients. A gastrinoma can be in the pancreas, and are located in the duodenum in 40% to 50% of patients. When located in the duodenum, gastrinomas are frequently small and multiple. The sensitivity of EUS is higher for a pancreatic gastrinoma than an extrapancreatic gastrinoma, probably because of their size. EUS also can detect adjacent metastatic lymph nodes within the gastrinoma triangle. Contrast-enhanced EUS (CE-EUS) increases the potential for detection of small pancreatic tumors by their ability to detect hypervascular enhancement [50, 51, 52]. The vast majority of small PNETs are predominantly hypoechogenic in B-mode (94%) and demonstrate hyperenhancement compared to the surrounding pancreatic parenchyma after contrast injection (90%).

EUS is also used to survey patients at an increased risk of developing PNETs, particularly in MEN type 1. A prospective multi-center study in 90 patients with MEN type 1 comparing MRI and pancreatic EUS showed that 48 (53%) of patients had at least one tumor over 10 mm. EUS detected 86 tumors over 10mm compared to 67 tumors for MRI. EUS failed to identify 16% of patients with pancreatic tumor over 10mm, and 19% patients for MRI. EUS and MRI should be compensated for each other. Both modalities should be performed at the initial evaluation of patients with MEN type 1.

Endoscopic Ultrasonography Guided Fine-Needle Aspiration (EUS-FNA)

Ability of EUS-FNA to Establish the Diagnosis of PNETs: A number of reports have described the excellent ability of EUS-FNA to establish the diagnosis of PNETS, with a sensitivity of 83% to 93% [53, 54, 55, 56]. EUS-FNA is essential for the preoperative diagnosis of PNETs. However, in about 10% to 15 % of patients, EUS-FNA is of little value [53, 54, 55, 56].

Size: Tumor size was not a significant predictor of adequate sampling. Tumors under 10mm were all diagnosed by EUS-FNA [57]. The reason for such a high yield may be the result of high cellularity and minimal stromal fibrosis in these tumors.

Tumor Location: Tumor location and the amount of intratumoral fibrosis were independent predictors of adequate sampling. Tumors located in the pancreatic body or tail was associated with greater sensitivity [58, 59].

Fibrosis: When tumors contain extensive stromal fibrosis (30%), EUS-FNA has a low diagnostic rate, compared to tumors with minimal fibrosis. Intratumoral fibrosis has been postulated to result from local serotonin production [60, 61], as serotonin has been implicated in fibrogenesis. In addition, serotonin has been shown to stimulate fibroblast mitosis in cell culture [62].

Most PNETs are hyper-intense on T2-WI. However, when PNETs have abundant stromal fibrosis, T2-W1 shows an isointense or hypointense pattern [63, 64]. Therefore, MRI should be performed when EUS-FNA for PNETs is planned. If an isointense or hypointense lesion is found on T2-WI, PNETs with rich fibrosis should be suspected. In such cases, tactics to obtain adequate tissue during EUS-FNA are required. CE-EUS may represent an attractive option in such cases to avoid sampling rich fibrous areas. Hypervascular sites in such lesions on CE-EUS are suitable for EUS-FNA [65]. When CE-EUS is not available, using high negative-pressure suction techniques in EUS-FNA [66-68] or using a larger gauge needle is useful options [55, 69].

False-Positives: False-positive results for PNETs have been reported. They include paraganglioma and pseudopapillary neoplasms (SPN). A report by Kari *et al.* [70] showed that 80% of lesions misclassified as PNETS were actually SPN. Usually, FNA samples demonstrate a pseudopapillary pattern with fibrovascular stalks in SPN. However, in some cases with material crushed during aspiration or inadequate sampling, characteristic features of SPN may not be evident. Additionally, chromogranin A and/or synaptophysin staining is sometimes positive in SPN [71].

Ohara *et al.* reviewed 30 surgical specimens of NETs (24 cases) and SPN (6 cases). They carried out

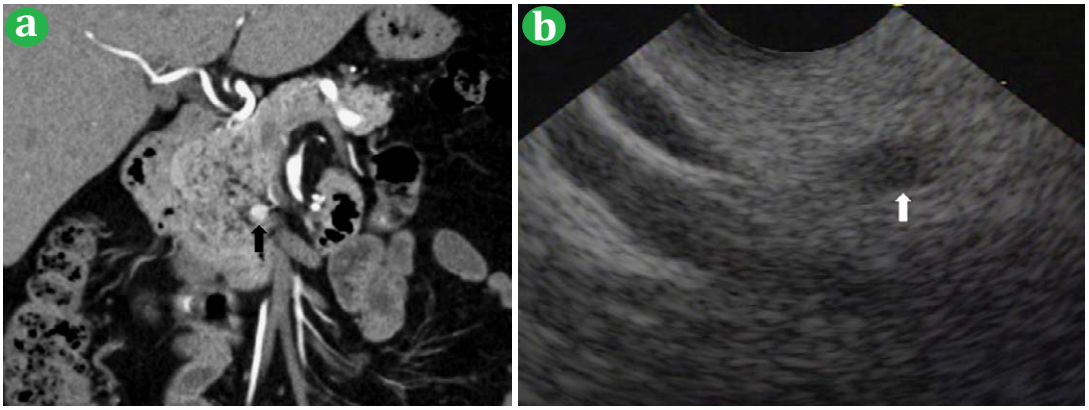

Figure 5. Tumor detected by Endoscopic ultrasound (Non-functioning tumor, G1). **(a).** Dynamic computed tomography scan shows a slightly hyper-vascular mass. **(b).** Endoscopic ultrasound shows a small hyperechoic tumor with well circumscribed margins.

comprehensive immunohistochemical profiling using 9 markers: synaptophysin, chromogranin A, pan-cytokeratin, E-cadherin, progesterone receptor, vimentin, α-1-antitrypsin, CD10, and β-catenin. E-cadherin staining in NETs, and nuclear labeling of β-catenin in SPNs were the most sensitive and specific markers. Dot-like staining of chromogranin A might indicate the possibility of SPNs rather than NETs. The other six markers were not useful because their expression overlapped widely between NETs and SPNs [72].

The remaining lesions misdiagnosed as PNETs are paraganglioma [73]. In the case of paraganglioma, EUS-FNA is relatively contraindicated because it may cause a severe hypertensive crisis during EUS-FNA [74]. Therefore, when paraganglioma is suspected, meta-iodobenzylguanidine (MIBG) scintigraphy and/or 24-h urine collection for catecholamines, metanephrines, and vanillylmandelic acid should be conducted before FNA [75].

Grading: The 2010 revised World Health Organization classification grades PNETs as NET-G1 G2 and NEC, based on Ki-67 staining or mitosis rates. Concordance rates between grading of PNETs by EUS-FNA sample and postoperative histology are 77% to 89.5% [76, 77, 78, 79, 80, 81].

As for PNET grading, some previous studies have shown that the Ki-67 index by EUS-FNA sample correlates significantly and independently with the clinical outcome of patients with PNETs [55, 82, 83, 84]. However, other authors have emphasized that metastases can also appear in PNETs with a low Ki-67 index by cytological or histological samples [85, 86].

The use of EUS-FNA samples for PNET grading has several limitations. As in surgical samples, the Ki-67 index from cytological samples can be calculated either in hot spot areas or can be estimated by dividing all positive tumor cells by total tumor cells in the smear. However, PNETs are heterogeneous tumors and the identification of hotspot areas in FNA specimens is difficult. FNA sample size is limited and cannot represent all tumor zones. Therefore, hotspot areas can be overlooked [77, 78, 85]. G2 tumors are particularly noted for their heterogeneity, and these tumors account for most of the discrepant cases. Authors who have correlated Ki-67 index in cytological and tissue samples have found both under-staging and upstaging of PNETS in cytological specimens, although under-staging has been more frequent [77].

As for the size of the lesions, Unno *et al.* found that there was a significant difference in tumor size in cases with concordant and discordant Ki-67 indices. When the tumor is large, the Ki-67 index obtained from EUS-FNA and surgical samples show a discrepancy [80]. They propose a tumor size of 18 mm as a cutoff to improve reliability of Ki-67 estimation in cytological samples.

In summary, PNETs with higher Ki-67 index from cytology specimens have a tendency towards a worse outcome. However, some patients with tumors classified as G1 on EUS-FNA samples died due to PNETs or had tumor progression. On cytological sample, a G2/G3 result presumably suggests worse prognosis, but a G1 result does not necessarily suggest a good outcome [86].

Endoscopic Retrograde Cholangiopancreatography (ERCP)

In typical PNETs, pancreatography has normal findings or shows only displacement of the main pancreatic duct (MPD). Usually duct obstruction is common in adenocarcinoma of the pancreas, and the intraductal growth of PNETs with narrowing or occlusion of MPD is rare. Fibrosis and compression by the tumor result in narrowing, and invasion or occupation of the tumor occur with occlusion of the MPD [87] **(Figure 6)**. Since the prognosis of patients with PNETs within the lumen of the MPD is worse compared to typical PNETs [88], endoscopic retrograde cholangiopancreatography (ERCP) is useful to predict the prognosis of patients with PNETs. In patients with PNETs invading the pancreatic duct, poorly differentiated intraductal adenocarcinoma (IDA)s may transform into NECs [89].

In patients with intraductal papillary mucinous neoplasms (IPMN) of the pancreas, pancreatic endocrine neoplasms may arise as well as intraductal papillary mucinous carcinoma (IPMC) and ductal adenocarcinoma [90]. When ERCP shows intraductal growth of tumor, anaplastic-type pancreatic adenocarcinoma and acinar cell carcinoma must be considered as well as NETs [91, 92, 93, 94, 95].

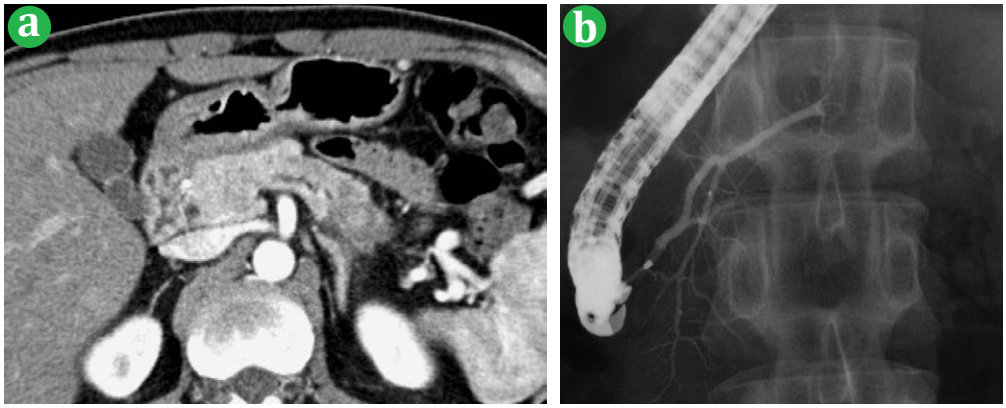

Figure 6. Tumor occupying the pancreatic duct. This lesion has a worse prognosis. (Non-functional tumor, NEC). **(a).** Dynamic computed tomography scan shows a hypo-enhanced tumor in the pancreatic duct. **(b).** Endoscopic retrograde cholangiopancreatography also shows a filling defect in the pancreatic duct.

CONCLUSION

Neuroendocrine tumors of the pancreas are a heterogeneous group of neoplasms that are generally slow growing. However, they may become incurable if they progress to unresectable metastatic disease. A combination of US, CT scan, MRI, radiopharmaceutical imaging techniques, and endoscopic techniques are useful for the diagnosis and grading of patients with PNETs.

Conflict of Interest

All authors declare having no conflict of interests.

References

1. Billimoria KY, Tomlinson JS, Merkow RP, Stewart AK, Ko CY, Talamonti MS, et al. Clinicopathologic features and treatment trends of pancreatic neuroendocrine tumors: analysis of 9821 patients. J Gastrointest Surg 2007; 11:1460-1467. [PMID: 17846854]

2. Yao JC, Hassan M, Phan A, Dagohoy C, Leary C, Mares JE, et al. One hundred years after ''carcinoid'': epidemiology of and prognostic factors for neuroendocrine tumors in 35,825 cases in the United States. J Clin Oncol 2008; 26:3063-3072. [PMID: 18565894]

3. Tsikitis VL, Wertheim BC, Guerrero MA. Trends of incidence and survival of gastrointestinal neuroendocrine tumors in the United States:a seer analysis. J Cancer 2012; 3:292-302. [PMID: 22773933]

4. Oshikawa O, Tanaka S, Ioka T, Nakaizumi A, Hamada Y, Mitani T. Dynamic sonography of pancreatic tumors: comparison with dynamic CT. AJR Am J Roentgenol 2002; 178:1133-1137. [PMID: 11959716]

5. Del Prete M, Di Sarno A, Modica R, Lassandro F, Giorgio A, Bianco A, et al. Role of contrast-enhanced ultrasound to define prognosis and predict response to biotherapy in pancreatic neuroendocrine tumors. J Endocrinol Invest 2017. [Epub ahead of print] [PMID: 28667452]

6. Fidler JL, Fletcher JG, Reading CC, Andrews JC, Thompson GB, Grant CS, et al. Preoperative detection of pancreatic insulinomas on multiphasic helical CT. AJR Am J Roentgenol 2003; 181:775-780. [PMID: 12933480]

7. Paulson EK, McDermott VG, Keogan MT, DeLong DM, Frederick MG, Nelson RC. Carcinoid metastases to the liver: role of triple-phase helical CT. Radiology 1998; 206:143-150. [PMID: 9423664]

8. Dromain C, de Baere T, Baudin E, Galline J, Ducreux M, Boige V, et al. MR imaging of hepatic metastases caused by neuroendocrine tumors: comparing four techniques. AJR Am J Roentgenol 2003; 180:121-128. [PMID: 12490490]

9. Dromain C, de Baere T, Lumbroso J, Caillet H, Laplanche A, Boige V, et al. Detection of liver metastases from endocrine tumors:a prospective comparison of somatostatin receptor scintigraphy, computed tomography, and magnetic resonance imaging. J Clin Oncol 2005; 23:70-78. [PMID: 15625361]

10. Ichikawa T, Peterson MS, Federle MP, Baron RL, Haradome H, Kawamori Y, et al. Islet cell tumor of the pancreas:biphasic CT versus MR imaging in tumor detection. Radiology 2000; 216:163-171. [PMID: 10887243]

11. Sheth S, Hruban RK, Fishman EK. Helical CT of islet cell tumor of the pancreas: typical and atypical manifestation. AJR Am J Roentgenol 2002; 179:725-730. [PMID: 12185053]

12. Gallotti A, Johnston RP, Bonaffini PA, Ingkakul T, Deshpande V, Fernández-del Castillo C, et al. Incidental neuroendocrine tumors of the pancreas:MDCT findings and features of malignancy. AJR Am J Roentgenol 2013; 200:355-362. [PMID: 23345357]

13. Kang TW, Kim SH, Lee J, Kim AY, Jang KM, Choi D, et al. Differentiation between pancreatic metastases from renal cell carcinoma and hypervascular neuroendocrine tumour: Use of relative percentage washout value and its clinical implication. Eur J Radiol 2015; 84:2089-2096. [PMID: 26318820]

14. Worhunsky DJ, Krampitz GW, Poullos PD, Visser BC, Kunz PL, Fisher GA, et al. Pancreatic neuroendocrine tumours: hypoenhancement on arterial phase computed tomography predicts biological aggressiveness. HPB(Oxford) 2014; 16:304-311. [PMID: 23991643]

15. Palazzo M, Lombard-Bohas C, Cadiot G, Matysiak-Budnik T, Rebours V, Vullierme MP, et al. Ki67 proliferation index, hepatic tumor load, and pretreatment tumor growth predict the antitumoral efficacy of lanreotide in patients with malignant digestive neuroendocrine tumors. Eur J Gastroenterol Hepatol 2013; 25:232-238. [PMID: 23108416]

16. Durante C, Boukheris H, Dromain C, Duvillard P, Leboulleux S, Elias D, et al. Prognostic factors influencing survival from metastatic (stage IV) gastroenteropancreatic well-differentiated endocrine carcinoma. Endocr Relat Cancer 2009; 16:585-597. [PMID: 19240182]

17. Bhosale P, Shah A, Wei W, Varadhachary G, Johnson V, Shah V, et al. Carcinoid tumours:predicting the location of the primary neoplasm based on the sites of metastases. Eur Radiol 2013; 23:400-407. [PMID: 22932740]

18. Leboulleux S, Dromain C, Vataire AL, Malka D, Aupérin A, Lum- broso J, et al. Prediction and diagnosis of bone metastases in well-differentiated gastro-entero-pancreatic endocrine cancer:a prospective comparison of whole body magnetic resonance imaging and somatostatin receptor scintigraphy. J Clin Endocrinol Metab 2008; 93:3021-3028. [PMID: 18522978]

19. Panzuto F, Falconi M, Nasoni S, Angeletti S, Moretti A, Bezzi M, et al. Staging of digestive endocrine tumours using helical computed tomography and somatostatin receptor scintigraphy. Ann Oncol 2003; 14:586-591. [PMID: 12649106]

20. D'Assignies G, Fina P, Bruno O, Vullierme MP, Tubach F, Paradis V, et al. High sensitivity of diffusion-weighted MR imaging for the detection of liver metastases from neuroendocrine tumors:comparison with T2-weighted and dynamic gadolinium-enhanced MR imaging. Radiology 2013; 268:390-399. [PMID: 23533288]

21. Caramella C, Dromain C, De Baere T, Boulet B, Schlumberger M, Ducreux M, et al. Endocrine pancreatic tumors:which are the most useful MRI sequences? Eur Radiol 2010; 20:2618-2627. [PMID: 20668861]

22. Brenner R, Metens T, Bali M, Demetter P, Matos C. Pancreatic neuroendocrine tumor: added value of fusion of T2-weighted imaging and high b-value diffusion-weighted imaging for tumor detection. Eur J Radiol 2012; 81:e746-749. [PMID: 22386133]

23. Manfredi R, Bonatti M, Mantovani W, Graziani R, Segala D, Capelli P, et al. Non-hyperfunctioning neuroendocrine tumours of the pancreas:MR imaging appearance and correlation with their biological behaviour. Eur Radiol 2013; 23:3029-3039. [PMID: 23793519]

24. Kim JH, Eun HW, Kim YJ, Lee JM, Han JK, Choi BI. Pancreatic neuroendocrine tumour (PNETS): staging accuracy of MDCT and its diagnostic performance for the differentiation of PNETS with uncommon CT findings from pancreatic adenocarcinoma. Eur Radiol 2016; 26:1338-1347. [PMID: 26253257]

25. Elias D, Lefevre JH, Duvillard P, Goéré D, Dromain C, Dumont F, et al. Hepatic metastases from neuroendocrine tumors with a ''thin slice'' pathological examination: they are many more than you think. Ann Surg 2010; 251:307-310. [PMID: 20010089]

26. Moryoussef F, de Mestier L, Belkebir M, Deguelte-Lardière S, Brixi H, Kianmanesh R, et al. Impact on management of liver and whole-body diffusion-weighted magnetic resonance imaging sequences for neuroendocrine tumors: a pilot study. Neuroendocrinology 2017; 104:264-272. [PMID: 27120316]

27. Papotti M, Bongiovanni M, Volante M, Allìa E, Landolfi S, Helboe L, et al. Expression of somatostatin receptor types 1-5 in 81 cases of gastrointestinal and pancreatic endocrine tumors. A correlative immunohistochemical and reverse- transcriptase polymerase chain reaction analysis. Virchows Arch 2002; 440:461-475. [PMID: 12021920]

28. Alexander HR, Fraker DL, Norton JA, Bartlett DL, Tio L, Benjamin SB, et al. Prospective study of somatostatin receptor scintigraphy and its effect on operative outcome in patients with Zollinger-Ellison syndrome. Ann Surg 1998; 228:228-238. [PMID: 9712569]

29. Abgral R, Leboulleux S, Déandreis D, Aupérin A, Lumbroso J, Dromain C, et al. Performance of (18)fluorodeoxyglucose-positron emission tomography and somatostatin receptor scintigraphy for high Ki67 (≥ 10%) well-differentiated endocrine carcinoma staging. J Clin Endocrinol Metab 2011; 96:665-671. [PMID: 21193541]

30. Garin E, Le Jeune F, Devillers A, Cuggia M, de Lajarte-Thirouard AS, Bouriel C, et al. Predictive value of 18F-FDG PET and somatostatin receptor scintigraphy in patients with metastatic endocrine tumors. J Nucl Med 2009; 50:858-864. [PMID: 19443590]

31. Montravers F, Grahek D, Kerrou K, Ruszniewski P, de Beco V, Aide N, et al. Can fluorodihydroxyphenylalanine PET replace somatostatin receptor scintigraphy in patients with digestive endocrine tumors? J Nucl Med 2006; 47:1455-1462. [PMID: 16954553]

32. Ambrosini V, Tomassetti P, Castellucci P, Campana D, Montini G, Rubello D, et al. Comparison between 68Ga-DOTA-NOC and 18F-DOPA PET for the detection of gastro-entero-pancreatic and lung neuro-endocrine tumours. Eur J Nucl Med Mol Imaging 2008; 35:1431-1438. [PMID: 18418596]

33. Haug A, Auernhammer CJ, Wängler B, Tiling R, Schmidt G, Göke B, et al. Intraindividual comparison of 68Ga-DOTA- TATE and 18F-DOPA PET in patients with well-differentiated metastatic neuroendocrine tumours. Eur J Nucl Med Mol Imaging 2009; 36:765-770. [PMID: 19137293]

34. Gabriel M, Decristoforo C, Kendler D, Dobrozemsky G, Heute D, Uprimny C, et al. 68Ga-DOTA-Tyr3-octreotide PET in neuroendocrine tumors:comparison with somatostatin receptor scintigraphy and CT. J Nucl Med 2007; 48:508-518. [PMID: 17401086]

35. Schmid-Tannwald C, Schmid-Tannwald CM, Morelli JN, Neumann R, Haug AR, Jansen N, et al. Comparison of abdominal MRI with diffusion-weighted imaging to 68Ga-DOTATATE PET/CT in detection of neuroendocrine tumors of the pancreas. Eur J Nucl Med Mol Imaging 2013; 40:897-907. [PMID: 23460395]

36. Putzer D, Gabriel M, Henninger B, Kendler D, Uprimny C, Dobrozemsky G, et al. Bone metastases in patients with neuroendocrine tumor:68 Ga-DOTA-Tyr3-octreotide PET in comparison to CT and bone scintigraphy. J Nucl Med 2009; 50:1214-1221. [PMID: 19617343]

37. Ambrosini V, Nanni C, Zompatori M, Campana D, Tomassetti P, Castellucci P, et al. (68)Ga-DOTA-NOC PET/CT in comparison with CT for the detection of bone metastasis in patients with neuroendocrine tumours. Eur J Nucl Med Mol Imaging 2010; 37:722-727. [PMID: 20107793]

38. Sadowski SM, Neychev V, Millo C, Shih J, Nilubol N, Herscovitch P, et al. Prospective study of 68Ga-DOTATATE positron emission tomography/computed tomography for detecting gastro-entero-pancreatic neuroendocrine tumors and unknown primary sites. J Clin Oncol 2016; 34:588-596. [PMID: 26712231]

39. Montravers F, Kerrou K, Nataf V, Huchet V, Lotz JP, Rusz-niewski P, et al. Impact of fluorodihydroxyphenylalanine-18F positron emission tomography on management of adult patients with documented or occult digestive endocrine tumors. J Clin Endocrinol Metab 2009; 94:1295-1301. [PMID: 19141589]

40. Tessonnier L, Sebag F, Ghander C, De Micco C, Reynaud R, Palazzo FF, et al. Limited value of 18F-F-DOPA PET to localize pancreatic insulin-secreting tumors in adults with hyperinsulinemic hypoglycemia. J Clin Endocrinol Metab 2010; 95:303-307. [PMID: 19915018]

41. Orlefors H, Sundin A, Garske U, Juhlin C, Oberg K, Skogseid B, et al. Whole-body (11)C-5-hydroxytryptophan positron emission tomography as a universal imaging technique for neuroendocrine tumors:comparison with somatostatin receptor scintigraphy and computed tomography. J Clin Endocrinol Metab 2005; 90:3392-3400. [PMID: 15755858]

42. Neels OC, Koopmans KP, Jager PL, Vercauteren L, van Waarde A, Doorduin J, et al. Manipulation of [11C]-5-hydroxytryptophan and 6-[18F] fluoro-3,4-dihydroxy-L-phenylalanine accumulation in neuroendocrine tumor cells. Cancer Res 2008; 68:7183-7190. [PMID: 18757434]

43. Imperiale A, Sebag F, Vix M, Castinetti F, Kessler L, Moreau F, et al. 18F-FDOPA PET/CT imaging of insulinoma revisited. Eur J Nucl Med Mol Imaging 2015; 42:409-418. [PMID: 25367749]

44. Imperiale A, Bahougne T, Goichot B, Bachellier P, Ta¨ıeb D, Namer IJ. Dynamic 18F-FDOPA PET findings after carbidopa premedication in 2 adult patients with insulinoma-related hyperinsulinemic hypoglycemia. Clin Nucl Med 2015; 40:682-684. [PMID: 25549347]

45. Helali M, Addeo P, Heimburger C, Detour J, Goichot B, Bachellier P, et al. Carbidopa-assisted 18F-fluorodihydroxyphenylalanine PET/CT for the localization and staging of non-functioning neuroendocrine pancreatic tumors. Ann Nucl Med 2016; 30:659-668. [PMID: 27485404]

46. van Asselt SJ, Brouwers AH, van Dullemen HM, van der Jagt EJ, Bongaerts AH, Kema IP, et al. EUS is superior for detection of pancreatic lesions compared with standard imaging in patients with multiple endocrine neoplasia type 1. Gastrointest Endosc 2015; 81:159-167. [PMID: 25527055]

47. Sotoudehmanesh R, Hedayat A, Shirazian N, Shahraeeni S, Ainechi S, Zeinali F, et al. Endoscopic ultrasonogrphy (EUS) in the localization of insulinoma. Endocrine 2007; 31:238-241. [PMID: 17906369]

48. Thomas-Marques L, Murat A, Delemer B, Penfornis A, Cardot-Bauters C, Baudin E, et al. Prospective endoscopic ultrasonographic evaluation of the frequency of nonfunctioning pancreaticoduodenal endocrine tumors in patients with multiple endocrine neoplasia type 1. Am J Gastroenterol 2006; 101:266-273. [PMID: 16454829]

49. Kann PH, Moll R, Bartsch D, Pfützner A, Forst T, Tamagno G, et al. Endoscopic ultrasound-guided fine-needle aspiration biopsy (EUS-FNA) in insulinomas:Indications and clinical relevance in a single investigator cohort of 47 patients. Endocrine 2017; 56:158-163. [PMID: 27905047]

50. Kitano M, Kudo M, Yamao K, Takagi T, Sakamoto H, Komaki T, et al. Characterization of small solid tumors in the pancreas:the value of contrast-enhanced harmonic endoscopic ultrasonography. Am J Gastroenterol 2012; 107:303-310. [PMID: 22008892]

51. Braden B, Jenssen C, D'Onofrio M, Hocke M, Will U, Möller K, et al. B-mode and contrast-enhancement characteristics of small nonincidental neuroendocrine pancreatic tumors. Endosc Ultrasound 2017; 6:49-54. [PMID: 28218201]

52. Barbe C, Murat A, Dupas B, Ruszniewski P, Tabarin A, Vullierme MP, et al. Magnetic resonance imaging versus endoscopic ultrasonography for the detection of pancreatic tumours in multiple endocrine neoplasia type 1. Dig Liver Dis 2012; 44:228-234. [PMID: 22078814]

53. Gornals J, Varas M, Catala I, Maisterra S, Pons C, Bargalló D, et al. Definitive diagnosis of neuroendocrine tumors using fine-needle aspiration-puncture guided by endoscopic ultrasonography. Rev Esp Enferm Dig 2011; 103:123-128. [PMID: 21434714]

54. Pais SA, Al-Haddad M, Mohamadnejad M, Leblanc JK, Sherman S, McHenry L, et al. EUS for pancreatic neuroendocrine tumors:a single-center, 11-year experience. Gastrointest Endosc 2010; 71:1185-1193. [PMID: 20304401]

55. Larghi A, Capurso G, Carnuccio A, Ricci R, Alfieri S, Galasso D, et al. Ki-67 grading of nonfunctioning pancreatic neuroendocrine tumors on histologic samples obtained by EUS-guided fine-needle tissue acquisition:a prospective study. Gastrointest Endosc 2012; 76:570-577. [PMID: 22898415]

56. Atiq M, Bhutani MS, Bektas M, Lee JE, Gong Y, Tamm EP, et al. EUS-FNA for pancreatic neuroendocrine tumors:a tertiary cancer center experience. Dig Dis Sci 2012; 57:791-800. [PMID: 21964743]

57. Hijioka S, Hara K, Mizuno N, Imaoka H, Bhatia V, Mekky MA, et al. Diagnostic performance and factors influencing the accuracy of EUS-FNA of pancreatic neuroendocrine neoplasms. J Gastroenterol 2016; 51:923-930. [PMID: 26768605]

58. Haba S, Yamao K, Bhatia V, Mizuno N, Hara K, Hijioka S, et al. Diagnostic ability and factors affecting accuracy of endoscopic ultrasound-guided fine needle aspiration for pancreatic solid lesions:Japanese large single center experience. J Gastroenterol 2013; 48:973-981. [PMID: 23090002]

59. Nakai Y, Isayama H, Chang KJ, Yamamoto N, Hamada T, Uchino R, et al. Slow pull versus suction in endoscopic ultrasound-guided fine-needle aspiration of pancreatic solid masses. Dig Dis Sci 2014; 59:1578-1585. [PMID: 24429514]

60. McCall CM, Shi C, Klein AP, Konukiewitz B, Edil BH, Ellison TA, et al. Serotonin expression in pancreatic neuroendocrine tumors correlates with a trabecular histologic pattern and large duct involvement. Hum Pathol 2012; 43:1169-1176. [PMID: 22221702]

61. Shi C, Siegelman SS, Kawamoto S, Wolfgang CL, Schulick RD, Maitra A, et al. Pancreatic duct stenosis secondary to small endocrine neoplasms:a manifestation of serotonin production? Radiology 2010; 257:107-114. [PMID: 20713615]

62. Lee SL, Wang WW, Lanzillo JJ, Fanburg BL. Serotonin produces both hyperplasia and hypertrophy of bovine pulmonary artery smooth muscle cells in culture. Am J Physiol 1994; 266:L46–52. [PMID: 8304469]

63. Thoeni RF, Mueller-Lisse UG, Chan R, Do NK, Shyn PB. Detection of small, functional islet cell tumors in the pancreas: selection of MR imaging sequences for optimal sensitivity. Radiology 2000; 214:483-490. [PMID: 10671597]

64. Lewis RB, Lattin GE Jr, Paal E. Pancreatic endocrine tumors: radiologic-clinicopathologic correlation. Radiographics 2010; 30:1445-1464. [PMID: 21071369]

65. Kitano M, Kamata K, Imai H, Miyata T, Yasukawa S, Yanagisawa A, et al. Contrast-enhanced harmonic endoscopic ultrasonography for pancreatobiliary diseases. Dig Endosc 2015; 27(Suppl 1):60-67. [PMID: 25639788]

66. Kudo T, Kawakami H, Hayashi T, Yasuda I, Mukai T, Inoue H, et al. High and low negative pressure suction techniques in EUS-guided fine-needle tissue acquisition by using 25-gauge needles: a multicenter, prospective, randomized, controlled trial. Gastrointest Endosc 2014; 80:1030-1037. e1. [PMID: 24890422]

67. Puri R, Vilmann P, Saftoiu A, Skov BG, Linnemann D, Hassan H, et al. Randomized controlled trial of endoscopic ultrasound-guided fine-needle sampling with or without suction for better cytological diagnosis. Scand J Gastroenterol 2009; 44:499-504. [PMID: 19117242]

68. Kawakami H, Kubota Y, Sakamoto N. Endoscopic ultrasound- guided fine-needle aspiration of gastrointestinal and pancreatic tumors: is negative pressure helpful or does it suck? Dig Dis Sci 2016; 61:660-662. [PMID: 26462486]

69. Sakamoto H, Kitano M, Komaki T, Noda K, Chikugo T, Dote K, et al. Prospective comparative study of the EUS guided 25-gauge FNA needle with the 19-gauge Trucut needle and 22-gauge FNA needle in patients with solid pancreatic masses. J Gastroenterol Hepatol 2009; 24:384-390. [PMID: 19032453]

70. Hooper K, Mukhtar F, Li S, Eltoum IA. Diagnostic error assessment and associated harm of endoscopic ultrasound-guided fine-needle aspiration of neuroendocrine neoplasms of the pancreas. Cancer Cytopathol 2013; 121:653-660. [PMID: 23839928]

71. Burford H, Baloch Z, Liu X, Jhala D, Siegal GP, Jhala N. E-cadherin/beta-catenin and CD10: a limited immunohistochemical panel to distinguish pancreatic endocrine neoplasm from solid pseudopapillary neoplasm of the pancreas on endoscopic ultrasound-guided fine-needle aspirates of the pancreas. Am J Clin Pathol 2009; 132:831-839. [PMID: 19926573]

72. Ohara Y, Oda T, Hashimoto S, Akashi Y, Miyamoto R, Enomoto T, et al. Pancreatic neuroendocrine tumor and solid-pseudopapillary neoplasm: Key immunohistochemical profiles for differential diagnosis. World J Gastroenterol 2016; 22:8596-8604. [PMID: 27784972]

73. Ganc RL, Castro ACF, Colaiacovo R, Vigil R, Rossini LG, Altenfelder R. Endoscopic ultra- sound-guided fine needle aspiration for the diagnosis of nonfunctional paragangliomas: a case report and review of the literature. Endosc Ultrasound 2012; 1:108-109. [PMID: 24949346]

74. Kubota K, Kato S, Mawatari H, Iida H, Akiyama T, Fujita K, et al. Risky endoscopic ultra- sonography-guided fine-needle aspiration for asymptomatic retroperitoneal tumors. Dig Endosc 2010; 22:144-146. [PMID: 20447211]

75. Baguet JP, Hammer L, Tremel F, Mangin L, Mallion JM. Metastatic phaeochromocytoma: risks of diagnostic needle puncture and treatment by arterial embolisation. J Hum Hypertens 2001; 15:209-211. [PMID: 11317207]

76. Carlinfante G, Baccarini P, Berretti D, Cassetti T, Cavina M, Conigliaro R, et al. Ki-67 cytological index can distinguish well-differentiated from poorly differentiated pancreatic neuroendocrine tumors:a comparative cytohistological study of 53 cases. Virchows Arch 2014; 465:49-55. [PMID: 24807732]

77. Farrell JM, Pang JC, Kim GE, Tabatabai ZL. Pancreatic neuroendocrine tumors: accurate grading with Ki-67 index on fine-needle aspiration specimens using the WHO 2010/ENETS criteria. Cancer Cytopathol 2014; 122:770-778. [PMID: 25044931]

78. Hasegawa T, Yamao K, Hijioka S, Bhatia V, Mizuno N, Hara K, et al. Evaluation of Ki-67index in EUS-FNA specimens for the assessment of malignancy risk in pancreatic neuroendocrine tumors. Endoscopy 2014; 46:32-38. [PMID: 24218309]

79. Remes SM, Tuominen VJ, Helin H, Isola J, Arola J. Grading of neuroendocrine tumors with Ki-67 requires high-quality assessment practices. Am J Surg Pathol 2012; 36:1359-1363. [PMID: 22895268]

80. Unno J, Kanno A, Masamune A, Kasajima A, Fujishima F, Ishida K, et al. The usefulness of endoscopic ultrasound-guided fine-needle aspiration for the diagnosis of pancreatic neuroendocrine tumors based on the World Health Organization classification. Scand J Gastroenterol 2014; 49:1367-1374. [PMID: 25180490]

81. Weynand B, Borbath I, Bernard V, Sempoux C, Gigot JF, Hubert C, et al. Pancreaticneuroendocrine tumour grading on endoscopic ultrasound-guided fine needle aspiration:high reproducibility and inter-observer agreement of the Ki-67 labelling index. Cytopathology 2014; 25:389-395. [PMID: 24750272]

82. Adsay V. Ki67 labeling index in neuroendocrine tumors of the gastrointestinal and pancreatobiliary tract: To count or not to count is not the question, but rather how to count. Am J Surg Pathol 2012; 36:1743-1746. [PMID: 23154766]

83. Alexiev BA, Darwin PE, Goloubeva O, Ioffe OB. Proliferative rate in endoscopic ultrasound fine-needle aspiration of pancreatic endocrine tumors: Correlation with clinical behavior. Cancer 2009; 117:40-45. [PMID: 19347828]

84. McCall CM, Shi C, Cornish TC, Klimstra DS, Tang LH, Basturk O, et al. Grading of well- differentiated pancreatic neuroendocrine tumors is improved by the inclusion of both Ki67 proliferative index and mitotic rate. Am J Surg Pathol 2013; 37:1671-1677. [PMID: 24121170]

85. Yang Z, Tang LH, Klimstra DS. Effect of tumor heterogeneity on the assessment of Ki67 labeling index in well-differentiated neuroendocrine tumors metastatic to the liver: Implications for prognostic stratification. Am J Surg Pathol 2011; 35:853-860. [PMID: 21566513]

86. Díaz Del Arco C, Esteban López-Jamar JM, Ortega Medina L, Díaz Pérez JÁ, Fernández Aceñero MJ. Fine-needle aspiration biopsy of pancreatic neuroendocrine tumors: Correlation between Ki-67 index in cytological samples and clinical behavior. Diagn Cytopathol 2017; 45:29-35. [PMID: 27863178]

87. Seki M, Ohta H, Ninomiya E, Aruga A, Murakami Y, Yanagisawa A, et al. Pancreatic endocrine tumor:pancreatographic features. Suizou (pancreas) 2001; 16:438-447. (Japanese).

88. Inagaki M, Watanabe K, Yoshikawa D, Suzuki S, Ishizaki A, Matsumoto K, et al. A malignant nonfunctioning pancreatic endocrine tumor with a unique pattern of intraductal growth. J Hepatobiliary Pancreat Surg 2007; 14:318-323. [PMID: 17520210]

89. Kimura T, Miyamoto H, Fukuya A, Kitamura S, Okamoto K, Kimura M, et al. Neuroendocrine carcinoma of the pancreas with similar genetic alterations to invasive ductal adenocarcinoma. Clin J Gastroenterol 2016; 9:261-265. [PMID: 27262570]

90. Goh BK, Ooi LL, Kumarasinghe MP, Tan YM, Cheow PC, Chow PK, et al. Clinicopathological features of patients with concomitant intraductal papillary mucinous neoplasm of the pancreas and pancreatic endocrine neoplasm. Pancreatology 2006; 6:520-526. [PMID: 17124434]

91. Okazaki M, Makino I, Kitagawa H, Nakanuma S, Hayashi H, Nakagawara H, et al. A case report of anaplastic carcinoma of the pancreas with remarkable intraductal tumor growth into the main pancreatic duct. World J Gastroenterol 2014; 20:852-856. [PMID: 24574758]

92. Hoshimoto S, Matsui J, Miyata R, Takigawa Y, Miyauchi J. Anaplastic carcinoma of the pancreas: Case report and literature review of reported cases in Japan. World J Gastroenterol 2016; 22:8631-8637. [PMID: 27784976]

93. Glazer ES, Neill KG, Frakes JM, Coppola D, Hodul PJ, Hoffe SE, et al. Systematic Review and Case Series Report of Acinar Cell Carcinoma of the Pancreas. Cancer Control 2016; 23:446-454. [PMID: 27842335]

94. Wang Y, Wang S, Zhou X, Zhou H, Cui Y, Li Q, et al. Acinar cell carcinoma: a report of 19 cases with a brief review of the literature. World J Surg Oncol 2016; 14:172. [PMID: 27352960]

95. Jakobsen M, Klöppel G, Detlefsen S. Mixed acinar-neuroendocrine carcinoma of the pancreas: a case report and a review. Histol Histopathol 2016; 31:1381-1388. [PMID: 27081013]